Origin of the Hydridic ^{1}H NMR Chemical Shift in Low-Valent Transition-Metal Hydrides

Yosadara Ruiz-Morales, Georg Schreckenbach, and Tom Ziegler*

Department of Chemistry, University of Calgary, Calgary, Alberta, Canada T2N 1N4

Received March 22, 1996[⊗]

We present a theoretical study of the ^{1}H NMR chemical shifts in low-valent transition metal hydrides based on density functional theory and gauge-including atomic orbitals (DFT-GIAO). Calculations have been carried out on the representative hydrides $HM(CO)_5$ (M = Mn, Tc, Re), $H_2Fe(CO)_4$, $HCo(CO)_4$, $[HCr(CO)_5]^-$, and $[HCr_2(CO)_{10}]^-$. In general, the calculated chemical shifts are in good agreement with the available experimental data. The paramagnetic and diamagnetic contributions to the ^{1}H chemical shielding have been analyzed in detail. Our calculations show that the paramagnetic current localized in the adjacent metal fragment, ML_n, is responsible for the negative "hydridic" shift observed in transition metal hydrides $H-ML_n$.

1. Introduction

Hydrogen atoms attached to metal centers are characterized[1,2] by a negative ^{1}H NMR chemical shift. The origin of this "hydridic" shift is not known with certainty. It is tempting to explain it in terms of an increase in the diamagnetic shielding as electron density is drawn from the metal center to the "hydridic" hydrogen. Alternatively, paramagnetic contributions from the adjacent metal fragment might be responsible for the shift, as has been suggested by Buckingham and Stephens[3] as early as 1964 in a qualitative discussion based on crystal field theory.

It has in the past decade become possible to carry out quantitative calculations on NMR chemical shifts.[4] We have recently presented a method in which the NMR shielding tensor is calculated by combining the "gauge-including atomic orbitals" (GIAO) approach with density functional theory (DFT).[5a] Recent investigations have shown that DFT is capable of reproducing ligand chemical shifts[5c,6,7] of transition-metal complexes. DFT can also reproduce metal chemical shifts of these compounds in a quantitative manner.[5c] The DFT-GIAO scheme has further been extended to include the frozen core approximation[5b] and the scalar relativistic two-component Pauli type Hamiltonian[5c] for relativistic calculations. Our implementation makes full use of the modern features of DFT in terms of accurate exchange-correlation (XC) energy functionals and large basis sets.

We present here DFT-GIAO calculations on the ^{1}H NMR chemical shift for the representative metal hydrides $HM(CO)_5$ (M = Mn, Tc, Re), $H_2Fe(CO)_4$, $HCo(CO)_4$, $[HCr(CO)_5]^-$, and $[HCr_2(CO)_{10}]^-$. The paramagnetic and diamagnetic contributions to the ^{1}H chemical shielding have been analyzed in detail with the objective of understanding the factors responsible for the observed hydridic ^{1}H NMR shift.

2. Computational Details

All calculations were based on the Amsterdam density functional package ADF.[8] This program has been developed by Baerends *et al.* and vectorized by Ravenek.[8e] The adopted numerical integration scheme was that developed by te Velde *et al.*[8f,8g]

The metal centers were described by an uncontracted triple-ζ STO basis set[9,10] for the outer *n*s, *n*p, *n*d, $(n+1)$s, and $(n+1)$p orbitals, whereas the shells of lower energy were treated by the frozen core approximation.[8a] The valence on carbon and oxygen included the 1s shell and was described by an uncontracted triple-ζ STO basis augmented by a single 3d and 4f function, corresponding to the basis set V of the ADF package.[8] A triple-ζ basis set augmented by two 2p polarization functions was employed for hydrogen. A number of auxiliary[11] s, p, d, f, and g STO functions, centered on all nuclei, were used in order to fit the molecular density and present Coulomb and exchange potentials accurately in each SCF cycle.

⊗ Abstract published in *Advance ACS Abstracts,* August 15, 1996.

(1) Jameson, C. J.; Mason, J. In *Multinuclear NMR*; Mason, J., Ed.; Plenum Press: New York, 1987; p 51.

(2) Elschenbroich, C.; Salzer, A. *Organometallics: A Concise Introduction,* 2nd ed.; Verlag Chemie: Weinheim, Germany, 1992.

(3) Buckingham, A. D.; Stephens, P. J. *J. Chem. Soc.* **1964**, 2747, 4583.

(4) (a) Kutzelnigg, W.; Fleischer, U.; Schindler, M. In *NMR-Basic Principles and Progress*; Springer-Verlag: Berlin, 1990; Vol. 23, p 165. (b) Tossell, J. A., Ed. *Nuclear Magnetic Shieldings and Molecular Structure*; *NATO Advanced Study Institute C386*; Kluwer Academic: Dordrecht, The Netherlands, 1993.

(5) (a) Schreckenbach, G.; Ziegler, T. *J. Phys. Chem.* **1995**, *99*, 606. (b) Schreckenbach, G.; Ziegler, T. *Int. J. Quantum Chem.* in press. (c) Schreckenbach, G.; Ziegler, T. *Int. J. Quantum Chem.*, in press.

(6) Ruiz-Morales, Y.; Schreckenbach, G.; Ziegler, T. *J. Phys. Chem.* **1996**, *100*, 3359.

(7) (a) Kaupp, M.; Malkin, V. G.; Malkina, O. L.; Salahub, D. R. *J. Am. Chem. Soc.* **1995**, *117*, 1851. (b) Kaupp, M.; Malkin, V. G.; Malkina, O. L.; Salahub, D. R. *Chem. Phys. Lett.* **1995**, *235*, 382. (c) Kaupp, M.; Malkin, V. G.; Malkina, O. L.; Salahub, D. R. *Chem. Eur. J.* **1996**, *2*, 24. (d) Kaupp, M. *Chem. Eur. J.* **1996**, *2*, 348. (e) Kaupp, M. *Chem. Ber.* **1996**, *129*, 527. (f) Kaupp, M. *Chem. Ber.* **1996**, *129*, 535.

(8) (a) Baerends, E. J.; Ellis, D. E.; Ros, P. *Chem. Phys.* **1973**, *2*, 41. (b) Baerends, E. J.; Ros, P. *Chem. Phys.* **1973**, *2*, 52. (c) Baerends, E. J.; Ros, P. *Int. J. Quantum Chem., Quantum Chem. Symp.* **1978**, *12*, 169. (d) te Velde, G. *Amsterdam Density Functional (ADF) User Guide, Release 1.1.3*; Department of Theoretical Chemistry, Free University: Amsterdam, The Netherlands, 1994. (e) Ravenek, W. In *Algorithms and Applications on Vector and Parallel Computers*; te Riele, H. J. J., Dekker, T. J., van de Horst, H. A., Eds.; Elsevier: Amsterdam, The Netherlands, 1987. (f) Boerrigter, P. M.; te Velde, G.; Baerends, E. J. *Int. J. Quantum Chem.* **1988**, *33*, 87. (g) te Velde, G.; Baerends, E. J. *J. Comput. Chem.* **1992**, *99*, 84.

(9) Snijders, J. G.; Baerends, E. J.; Vernoijs, P. *At. Nucl. Data Tables* **1982**, *26*, 483.

(10) Vernoijs, P.; Snijders, J. G.; Baerends, E. J. *Slater Type Basis Functions for the Whole Periodic System*; Internal Report (in Dutch); Department of Theoretical Chemistry, Free University: Amsterdam, The Netherlands, 1981.

(11) Krijn, J.; Baerends, E. J. *Fit Functions in the HFS Method*; Internal Report (in Dutch); Department of Theoretical Chemistry, Free University: Amsterdam, The Netherlands, 1984.

S0276-7333(96)00218-X CCC: $12.00

Table 1. Comparison of Experimental and Calculated ^{1}H Chemical shift for Transition Metal Hydrides

system	M−H dist (Å)	δ (ppm) calcd[a]	δ (ppm) exptl[b]
$[HCr(CO)_5]^-$	1.6609	−6.5[d]	−6.9[e]
$[HCr_2(CO)_{10}]^-$	1.722[j]	−20.3[d]	−19.5[f]
$HMn(CO)_5$	1.589[k]	−6.8[d]	−7.5[g]
$HTc(CO)_5$	1.620[n]	−5.7[d]	
$HRe(CO)_5$ rel[c]	1.620[l]	−5.2[c]	−5.7[g]
$H_2Fe(CO)_4$	1.5325	−7.5[d]	−11.1[h]
$HCo(CO)_4$	1.486[m]	−5.3[d]	−10.7[i]

[a] $\delta = \sigma_{TMS} - \sigma_{complex}$. All data are reported with respect to the calculated isotropic shielding constant $\sigma(^1H)$ of 30.99 ppm for TMS. The calculation was carried out assuming staggered T_d symmetry. The structural data were taken from ref 26. [b] Relative to TMS. [c] Relativistic NL-SCF-QR calculation. [d] Nonrelativistic NL-SCF calculation. [e] Reference 28. [f] References 28b and 29. [g] Reference 30. [h] Reference 19. [i] Reference 20. [j] Reference 31. [k] Reference 32. [l] Reference 16. [m] Reference 17. [n] Optimized structure.

The self-consistent DFT calculations were carried out by augmenting the local exchange-correlation potential of Vosko *et al.*[12] with Becke's[13] nonlocal exchange corrections and Perdew's[14] nonlocal correlation correction (NL-SCF). The 3d and 4d complexes were treated without considering relativistic effects whereas quasi-relativistic[15] (NL-SCF+QR) calculations were carried out for the 5d complex $Re(CO)_5H$. Optimized M−H bond lengths were adopted for all systems except for the case of $[HCr_2(CO)_{10}]^-$, for which the experimental structural data was used. The inclusion of the frozen core approximation[5b] and quasi-relativistic[5c] effects into the shielding calculations is described elsewhere.

3. Results and Discussion

Table 1 compares the calculated ^{1}H NMR chemical shifts for the metal hydrides with experimental estimates. The calculated shifts for the two isoelectronic hydrido pentacarbonyls of the first transition series are −6.8 ppm in the case of $HMn(CO)_5$ and −6.5 ppm for $[HCr(CO)_5]^-$, in good agreement with the experimental estimates of, respectively, −7.5 and −6.9 ppm. The homologous 5d system $HRe(CO)_5$[16] has a theoretical shift of −5.2 ppm, also in good agreement with the observed shift at −5.7 ppm.

Formally adding a $[Cr(CO)_5]$ fragment to $[HCr(CO)_5]^-$ results in the dinuclear species $[HCr_2(CO)_{10}]^-$, in which the hydride is bridged between the two metal centers. The calculated hydridic shift amounts to −20.3 ppm. It is more than twice as big as the shift of the monomer and agrees well with the measured shift of −19.5 ppm.

Our calculated shifts for $H_2Fe(CO)_4$ and $HCo(CO)_4$[17] of −7.5 and −5.3 ppm, respectively, are in line with the values predicted for the other mononuclear systems but differ from the experimental estimates of −11.1 and −10.7 ppm, respectively. Part of the discrepancy might be due to the instability of both hydrides[18−20] as well as to the fluxional behavior observed[21] for $H_2Fe(CO)_4$.

Origin of the Hydridic Shift. We shall now discuss the factors responsible for the strong negative "hydridic"

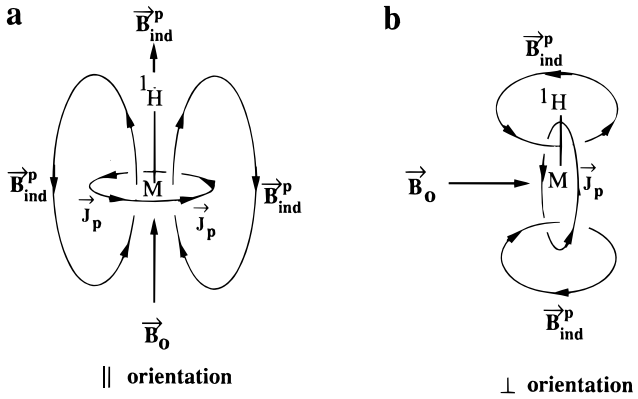

Figure 1. Schematic representations of the effect of the induced magnetic field at the position of the hydrogen atom.

^{1}H NMR chemical shift in low-valent transition-metal hydrides.

The isotropic ^{1}H chemical shielding, σ, can be written as a sum of one diamagnetic contribution, σ^d, and two paramagnetic contributions, $\sigma_\perp{}^p$ and $\sigma_\parallel{}^p$ according to[5a]

$$\sigma = \sigma^d + {}^1/_3\sigma_\parallel{}^p + {}^2/_3\sigma_\perp{}^p \quad (1)$$

This separation is well-defined within the GIAO scheme.[5a] The diamagnetic shielding, σ^d, stems from a circulation of the ground-state density around the ^{1}H probe induced by the applied magnetic field $\vec{B}_o$, as illustrated in standard textbooks. The circulation results in an induced magnetic field, $\vec{B}^d_{ind}$, which is opposite in direction to $\vec{B}_o$ irrespective of the orientation of the M−H bond relative to $\vec{B}_o$. The corresponding shielding, σ^d, is as a consequence positive. The diamagnetic shielding is usually the dominating factor in determining ^{1}H chemical shifts for main-group compounds.

The paramagnetic contributions are the result of a current density $\vec{J}_p$ induced by $\vec{B}_o$. The situation is shown in Figure 1a with the applied field $\vec{B}_o$ parallel to the M−H bond. The induced current density $\vec{J}_p$ stems from the coupling by $\vec{B}_o$ of orbitals which in the field-free case with $\vec{B}_o = 0$ either are occupied or are virtual. The orbitals involved reside primarily on the metal fragment adjacent to the ^{1}H probe, as discussed in detail later. The induced current density $\vec{J}_p$ moves in a plane perpendicular to $\vec{B}_o$ containing the metal center. The resulting magnetic field, $\vec{B}^p_{ind}$, is parallel to $\vec{B}_o$ "inside" the loop of the current density $\vec{J}_p$ and opposite in direction to $\vec{B}_o$ outside the loop (Figure 1a). With the M−H bond inside the current loop, the induced magnetic field $\vec{B}^p_{ind}$ is parallel to $\vec{B}_o$ and the corresponding shielding, $\sigma_\parallel{}^p$, is negative (Figure 1a). Similar paramagnetic currents have also been noted and discussed for organic molecules.[4a]

The situation where the applied field $\vec{B}_o$ is perpendicular to the M−H bond is shown in Figure 1b. Again, $\vec{B}_o$ will induce a current density $\vec{J}_p$ in a plane perpendicular to $\vec{B}_o$ containing the metal center. However, now

(12) Vosko, S. H.; Wilk, L.; Nusair, M. *Can. J. Phys.* **1980**, *58*, 1200.
(13) Becke, A. *Phys. Rev. A* **1988**, *38*, 3098.
(14) Perdew, J. *Phys. Rev. B* **1986**, *33*, 8822.
(15) (a) Snijders, J. G.; Baerends, E. J. *Mol. Phys.* **1978**, *36*, 1789. (b) Snijders, J. G.; Baerends, E. J.; Ros, P. *Mol. Phys.* **1979**, *38*, 1909. (c) Ziegler, T.; Tschinke, V.; Baerends, E. J.; Snijders, J. G.; Ravenek, W. *J. Phys. Chem.* **1989**, *93*, 3050.
(16) Ziegler, T.; Tschinke, V.; Becke, A. *J. Am. Chem. Soc.* **1987**, *109*, 1351−1358.
(17) Fan, L.; Ziegler, T. *J. Chem. Phys.* **1991**, *95*, 7401.
(18) Gingsberg, A. P. In *Transition Metal Chemistry*; Carlin, R. L., Ed.; Marcel Dekker: New York, 1965; Vol. 1.
(19) (a) Friedel, R. A.; Wender, I.; Shufler, S. L.; Sternberg, H. W. *J. Am. Chem. Soc.* **1955**, *77*, 3951. (b) Edgell, W. F.; Summitt, R. *J. Am. Chem. Soc.* **1961**, *83*, 1772.
(20) Cotton, F. A.; Wilkinson, G. *Chem. Ind.* **1956**, 1305.
(21) Vancea, L.; Graham, W. A. G. *J. Organomet. Chem.* **1977**, *134*, 219.

Table 2. Calculated Paramagnetic and Diamagnetic Contributions to the ^{1}H Chemical Shielding and ^{1}H Chemical Shift for Metal Hydrides (All Values in ppm)

system	σ^d	$\sigma_\perp^p$	$\sigma_\parallel^p$	σ^p	calcd σ (absolute shielding)[g]	total diamag contribn to the chem shift[f] δ^d	total paramag contribn to the chem shift[f] δ^p	total calcd chem shift[a] δ
H (atom)	16.8	0.0	0.0	0.0	16.8[d] (17.73[e])	13.2		14.2
H^-	25.3	0.0	0.0	0.0	25.3[d] (24.38[e])	4.7		5.7
TMS	30.00			0.99	30.99	0.0		
$[HCr(CO)_5]^-$	25.1	20.5	−3.8	12.4	37.5[d]	4.9	−11.4	−6.5
$[HCr_2(CO)_{10}]^-$	26.7	41.6[b]	−9.6	24.6	51.3[d]	3.3	−23.6	−20.3
$HMn(CO)_5$	23.2	24.9	−6.1	14.6	37.8[d]	6.8	−13.6	−6.8
$HTc(CO)_5$	24.9	18.8	−2.2	11.8	36.7[d]	5.1	−10.8	−5.7
$HRe(CO)_5$ rel	27.6	12.9	−0.1	8.6	36.2[c]	2.4	−7.6	−5.2
$H_2Fe(CO)_4$	25.6	23.1[h]	−7.4	12.9	38.5[d]	4.4	−11.9	−7.5
$HCo(CO)_4$	26.9	22.4	−16.5	9.4	36.3[d]	3.1	−8.4	−5.3

[a] $\delta = \sigma_{TMS} - \delta_{complex}$ or $\delta = \delta^d + \delta^p$. All data are reported with respect to calculated TMS; $\sigma(^1H) = 30.99$ ppm. The calculation was carried out assuming a staggered T_d symmetry. The structural data were taken from ref 26. [b] Although there is no axial symmetry present, $\sigma_\perp^p$ was calculated from $\sigma_\perp^p = {}^1/_2(\sigma_{xx} + \sigma_{yy})$. $\sigma_{xx}^p = 42.3$ ppm and $\sigma_{yy}^p = 40.9$ ppm. [c] Relativistic NL-SCF-QR calculation. [d] Nonrelativistic NL-SCF calculation. [e] Reference 27. [f] $\delta^d = \sigma_{TMS}^d - \sigma_{complex}^d$ and $\delta^p = \sigma_{TMS}^p - \sigma_{complex}^p$. [g] $\sigma = \sigma^d + \sigma^p$. [h] Although there is no axial symmetry present, $\sigma_\perp^p$ was calculated from $\sigma_\perp^p = {}^1/_2(\sigma_{xx} + \sigma_{yy})$. $\sigma_{xx}^p = 26.2$ ppm and $\sigma_{yy}^p = 20.0$ ppm.

the M−H bond is outside the current loop and the induced magnetic field $\vec{B}_{ind}^p$ is opposite to $\vec{B}_o$, resulting in a positive shielding $\sigma_\perp^p$. Any applied magnetic field is readily decomposed into components parallel or perpendicular to the M−H bond. The paramagnetic isotropic shielding is as a result determined by $\sigma_\perp^p$ and $\sigma_\parallel^p$ (Figure 1).

The ^{1}H chemical shift δ can in the present case be written as

$$\delta = \sigma_{TMS} - \sigma_{complex} \tag{2}$$

Note that the shielding, σ, and the chemical shift, δ, have opposite signs. It is further possible to write δ in terms of its diamagnetic, δ^d, and paramagnetic, δ^p, contributions as

$$\delta = \delta^d + \delta^p \tag{3}$$

where

$$\delta^d = \sigma_{TMS}^d - \sigma_{complex}^d \tag{4}$$

$$\delta^p = \sigma_{TMS}^p - \sigma_{complex}^p \cong -\sigma_{complex}^p \cong -{}^2/_3\sigma_\perp^p - {}^1/_3\sigma_\parallel^p \tag{5}$$

The positive contributions from $\sigma_\perp^p$ and σ^d to the isotropic shielding can both potentially give rise to the negative "hydridic" shift, whereas the negative $\sigma_\parallel^p$ term would have a positive contribution to the chemical shift. Table 2 displays our calculated diamagnetic and paramagnetic contributions to the chemical shielding and the chemical shift.

The calculated diamagnetic shieldings, σ^d, for the metal hydrides fall in the range 23.2−27.6 ppm (Table 2). These values are close to σ^d estimated[27] for the free hydride ion H^- of 24.38 ppm. They are even larger than the diamagnetic shielding[27] for the hydrogen atom at 17.73 ppm, as one would expect for a hydrogen which draws electron density from the less electronegative metal center. However, the diamagnetic shielding for the reference TMS is calculated to be as large as $\sigma^d = 30.00$ ppm. Hence, the diamagnetic shifts for the metal hydrides are all positive and they cannot be responsible for the "hydridic" shift.

The paramagnetic term $\sigma_\perp^p$ (Figure 1b) is seen to have a large positive contribution (Table 2), which according to eq 5 gives rise to a negative shift (see also Table 2). Thus, the "hydridic" isotropic shift in transition-metal hydrides is largely due to the paramagnetic current density induced in the ML_n fragment from the component of the external magnetic field perpendicular to the M−H bond (Figure 1b). The paramagnetic current density induced by the component parallel to the M−H bond affords a negative shielding $\sigma_\parallel^p$ (Figure 1a), which will reduce the "hydridic" shift (eq 5 and Table 2).

The dimeric $[HCr_2(CO)_{10}]^-$ system is especially interesting, since it gives rise to a paramagnetic chemical shift of −23.6 ppm, which in absolute terms is nearly twice as large as the calculated shift for $[HCr(CO)_5]^-$ with δ −11.4 ppm. This is understandable from our analysis, since the hydride in the dimer experiences additive induced magnetic fields from two metal fragments. This can easily be shown by drawing diagrams similar to those for the monomers in Figure 1. We shall now turn to a more detailed discussion of the separate systems and the orbitals responsible for the induced current densities.

Paramagnetic Coupling. The d^6 HML_5 systems have a pseudo-octahedral geometry. The occupied levels of highest energy are represented by the t_{2g} type d_π metal orbitals transforming as e_1 and b_2 in the C_{4v} point group symmetry of HML_5. The unoccupied levels of lowest energy are represented by the e_g type d_σ metal orbitals transforming as a_1 and b_1 in C_{4v} symmetry.

Our calculations reveal that the contribution to the $\sigma_\perp^p$ components (Table 2) mainly comes from the coupling between the occupied d_π-type e_1 orbitals (**1a**) and the virtual d_σ type a_1 orbital, (**lb**) through $\langle d_\pi(HOMO)|\hat{M}_s|d_\sigma\rangle$ (s = *x*, *y*),[22] where $\hat{M}_s$ is a component of the angular momentum operator.[23] The term $\hat{M}_y a_1(d_\sigma)$[24,25] (**1c**) will have the form of a π-type orbital, and thus it will overlap with the HOMO (**1a**) through

(22) For a more detailed description, see ref 6.

(23) The bracket notation $\langle\Psi_1|M_z|\Psi_2\rangle$ denotes certain matrix elements (integrals) between the two orbitals Ψ_1 and Ψ_2 that contribute to the paramagnetic shielding σ^p.

(24) The expression $\hat{M}_y a_1(d_\sigma)$ denotes an orbital resulting from the action of the operator $\hat{M}_y$ on the $a_1(d_\sigma)$ orbital.

(25) (a) Ballhause, C. J. *Introduction to Ligand Field Theory*; McGraw-Hill: New York, 1962; p 149. (b) McGlynn, S. P.; Vanquickenborne, L. G.; Kinoshita, M.; Carrol, D. G. In *Introduction to Applied Quantum Chemistry*; Holt, Rinehart and Winston: New York, 1972.

(26) Beagley, B.; Monaghan, J. J.; Hewitt, T. G. *J. Mol. Struct.* **1971**, *8*, 401.

(27) Mason, J. *J. Chem. Soc., Dalton Trans.* **1975**, 1422.

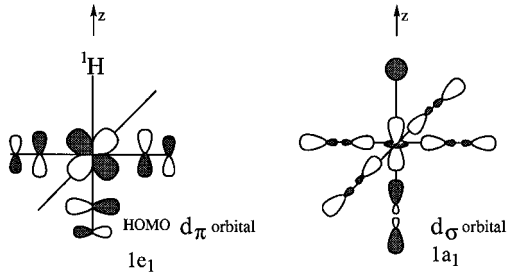

1a

1b

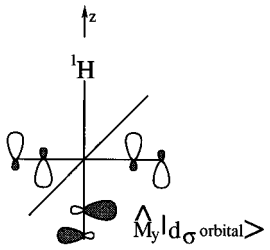

1c

the common lobes. The paramagnetic current induced by the coupling generates a magnetic field that exerts a net shielding effect on the hydrogen atom (Figure 1a).

The contributions to the $\sigma_{||}^p$ component of the shielding tensor comes from a coupling between the occupied d_π type b_2 orbital (**2a**) and the d_σ type virtual b_1 orbital (**2b**) through $\langle d_\pi(\text{HOMO})|\hat{M}_z|d\sigma\rangle$. The component, $\hat{M}_z d_\sigma$

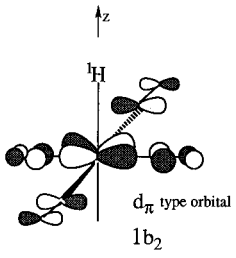

2a

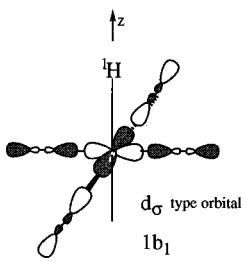

2b

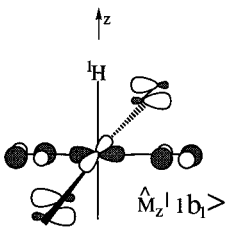

2c

(**2c**) will overlap with **2a**, through the common lobes. In this case the paramagnetic current induced by the coupling generates a magnetic field that exerts a net deshielding effect at the hydrogen atom (Figure 1b).

For the complex $[\mu\text{-}HCr_2(CO)_{10}]^-$, the type of coupling discussed above takes place in each of the two $[Cr(CO)_5]$ metal fragments (**1a**−**c** and **2a**−**c**). The induced fields from the two metal fragments add up, producing $\sigma_\perp^p$ and $\sigma_{||}^p$ components of double the size in absolute terms. Again, the positive $\sigma_\perp^p$ component is dominating and the total ^{1}H shift is negative.

The coupling mechanisms in $HCo(CO)_4$ and H_2FeCO_4 are quite similar to those discussed for the $HM(CO)_5$ systems. Again, π and σ type orbitals are involved in producing the induced paramagnetic current densities.

It is important to mention that we preferred to use fully optimized structures for the shielding calculations because the experimental structures[28a,33,34] have not all been determined with the same accuracy. The only exception was the larger dimer $[HCr_2(CO)_{10}]^-$. We find that the shifts calculated for experimental and optimized structures differ by less than 1 ppm. The only exception is $HRe(CO)_5$, where the difference was 3.2 ppm. Typically, an increase in R(M−H) by 0.05 Å would reduce the hydridic shift by 1 ppm.

4. Conclusions

We have applied the DFT-GIAO method to calculate the ^{1}H chemical shift in various metal hydrides of the type $HM(CO)_5$ (M = Mn, Tc, Re), $H_2Fe(CO)_4$, $HCo(CO)_4$, $[HCr(CO)_5]^-$, and $[HCr_2(CO)_{10}]^-$. We found that in general the results are in satisfactory agreement with the experimental data. The largest deviation was found in the case of $HCo(CO)_4$ and $H_2Fe(CO)_4$.

Paramagnetic contributions from the adjacent metal fragment are responsible for the observed "hydridic" ^{1}H chemical shift in metal hydrides, as already suggested by Buckingham and Stephens[3] in 1964. The role of the adjacent ML_n fragment is clearly demonstrated in the complex $[\mu\text{-}HCr_2(CO)_{10}]^-$, where the paramagnetic contribution to the ^{1}H chemical shift is almost double compared to the monomer systems, due to the superimposing of contributions from two metallic fragments.

The paramagnetic shielding tensor has two parts, $\sigma_{||}^p$ and $\sigma_\perp^p$. The last part, $\sigma_\perp^p$, stems from the component of the applied external field $\vec{B}_o$ which is perpendicular to the M−H bond. This component, $\vec{B}_\perp$, gives rise to an induced magnetic field $\vec{B}_{ind}^p$ which is opposite in direction to $\vec{B}_\perp$ (Figure 1a). Thus $\sigma_\perp^p$ is positive with a negative contribution to the ^{1}H chemical shift. The first paramagnetic shielding term, $\sigma_{||}^p$, comes from the component $\vec{B}_{||}$ of the applied magnetic field $\vec{B}_o$, which is parallel to the M−H bond. The component $\vec{B}_{||}$ induces a field $\vec{B}_{ind}^p$ in the same direction as $\vec{B}_{||}$ (Figure 1b). Thus, $\sigma_{||}^p$ is negative with a positive contribution to the ^{1}H shift. The component $\sigma_\perp^p$ is dominating and is responsible for the "hydridic" ^{1}H shift in low-valent transition-metal complexes.

Acknowledgment. This work has been supported by the Natural Sciences and Engineering Research Council of Canada (NSERC). G.S. is grateful to the Graduate Faculty Council, University of Calgary, for a scholarship, Y.R.-M. acknowledges a scholarship from DGAPA-UNAM (Mexico), and T.Z. acknowledges a Canada Council Killam Research Fellowship. We thank the donors of the Petroleum Research Fund (ACS-PRF-31205-AC3), administered by the ACS, for partial support of this research.

OM960218N

(28) (a) Darensbourg, M. Y.; Bau, R.; Marks, M. W.; Burch, R. R., Jr.; Deaton, J. C.; Slater, S. *J. Am. Chem. Soc.* **1982**, *104*, 6961. (b) Darensbourg, M. Y.; Deaton, J. C. *Inorg. Chem.* **1981**, *120*, 1644.
(29) Hayter, R. G. *J. Am. Chem. Soc.* **1966**, *88*, 4376.
(30) Davison, A.; McCleverty, J. A.; Wilkinson, G. *J. Chem. Soc.* **1963**, 1133.
(31) Roziere, J.; Williams, J. M.; Stewart, R. P., Jr.; Peterse, J. L.; Dahl, L. F. *J. Am. Chem. Soc.* **1977**, *99*, 4497.
(32) Folga, E.; Ziegler, T. *J. Am. Chem. Soc.* **1993**, *115*, 5169.
(33) McNeill, E. A.; Scholer, F. R. *J. Am. Chem. Soc.* **1977**, *99*, 6243.
(34) Kukolich, S. G.; Sickafoose, S. M. *J. Chem. Phys.* **1993**, *99*, 6465.